Published in final edited form as:
Organometallics. 2013 September 23; 32(18): . doi:10.1021/om4006966.

Investigations into Ruthenium Metathesis Catalysts with Six-Membered Chelating NHC Ligands: Relationship between Catalyst Structure and Stereoselectivity

Koji Endo, **Myles B. Herbert**, and **Robert H. Grubbs***
Arnold and Mabel Beckman Laboratory of Chemical Synthesis, Division of Chemistry and Chemical Engineering, California Institute of Technology, Pasadena, California 91125, United States

Abstract

A series of ruthenium catalysts bearing five-membered chelating NHC architectures that exhibit very high *Z*-selectivity in a variety of metathesis reactions have recently been reported. It was envisioned that catalysts possessing sixmembered chelates could similarly exhibit high *Z*-selectivity and address limitations of this methodology. We thus prepared a number of new catalysts and systematically investigated the impact of the NHC and anionic ligand on their stereoselectivity. In standard metathesis assays, only catalysts containing six-membered chelated NHC structures and η^2-bound anionic ligands favored the *Z*-olefin products compared to traditional ruthenium catalysts. In addition, substitution with bulkier *N*-aryl groups led to improved *Z*-selectivity. The effect of ligand structure on stereoselectivity discovered in this study will be useful in the future design of highly active and *Z*-selective ruthenium catalysts.

INTRODUCTION

Olefin metathesis is a convenient and powerful method for the construction of carbon-carbon double bonds, and is widely used in a variety of fields including natural product synthesis,[1] biochemistry,[2] green chemistry[3] and polymer chemistry.[4] Since its discovery in the 1950's, this methodology has developed at a fast pace due to the discovery of well-defined transition metal catalysts and advances in catalyst efficiency.[5] While molybdenum and tungsten catalysts initially gained popularity due to their high activity,[6] the discovery of highly active and functional group tolerant ruthenium catalysts has enabled the wide-spread use of this methodology in both academic laboratories and industry processes.[7]

Metathesis reactions generally proceed under thermodynamic control, meaning that most catalysts predominantly provide *E*-olefin products.[8] Recently, however, catalysts capable of preferentially forming the *Z*-isomer have been discovered. [9, 10, 11] The first breakthrough in this field was reported by the Hoveyda and Schrock groups.[9a] The reported monoaryloxidepyrrolide (MAP) molybdenum and tungsten catalysts provided a very high proportion of *cis*(*Z*)-olefin products in the homo-coupling of terminal olefins, and more complicated metathesis reactions.[9] This *Z*-selectivity was attributed to the difference in size of the two axial ligands in relevant metallacyclobutane intermediates. Based on this same

CORRESPONDING AUTHOR: rhg@caltech.edu.

ASSOCIATED CONTENT

Supporting Information. Experimental details, NMR spectra, and crystallographic data are available free of charge via the Internet at http://pubs.acs.org.

concept, Jensen and coworkers reported a ruthenium catalyst bearing a single bulky thiolate ligand that also achieved high *Z*-selectivity in olefin homocoupling.[10]

We have reported a series of ruthenium-based catalysts with unique chelating *N*-heterocyclic carbene (NHC) architectures (Figure 1).[11] Cross metathesis (CM) products formed using these catalysts had a significantly lower *E*/*Z* ratio compared to previous generations of ruthenium catalysts. NHC-chelated structures derived from ruthenium alkylidene complexes had been previously observed, however they were formed as decomposition products and were not metathesis active.[12] Catalysts **1a** and **2a-c** were synthesized via an intramolecular carboxylate-driven C-H bond insertion and contained an intact alkylidene. Complexes containing a five-membered chelate (**2a-c**) exhibited very high *Z*-selectivity in a variety of metathesis reactions including the homocoupling of terminal olefins, CM, macrocyclic ring-closing metathesis (RCM) and ring-opening metathesis polymerization (ROMP). This methodology has started to be applied to the synthesis of insect pheromones and more complicated natural products.[13] Recent density functional theory (DFT) calculations for catalysts **1a**, **2a** and **2b** suggest that reactions involving these chelated catalysts proceed under kinetic control through 'side-bound' ruthenacyclobutane intermediates. [14] It was proposed that the chelating NHC positions the *N*-aryl group above the ruthenacyclobutane, increasing the steric penalty for ruthenacycle substituents that point toward the *N*-aryl group and thus leading to productive formation of *Z*-olefins.

In order to design highly efficient *Z*-selective catalysts containing six-membered chelating architectures, a more thorough understanding of the influence of ligands on stereoselectivity and activity is of paramount importance. In this report, we have prepared and crystallographically characterized a number of new NHC-chelated and non-chelated catalysts, and subsequently tested their activity in a variety of metathesis reactions. In this way, we attempted to clarify the relationship between catalyst structure and stereoselectivity with this class of catalysts.

RESULTS and DISCUSSION

Catalyst Syntheses

Modifications to the non-chelating *N*-aryl group of chelated catalysts were achieved by straightforward ligand and catalyst synthesis (Figure 2). Complex **3**, bearing an *N*-Mes, *N*'-DIPP substituted NHC ligand, was reacted with silver pivalate, affording the bulkier NHC-chelated catalyst **4** (Scheme 1).[15] The salt metathesis and C-H activation was monitored by ^{1}H NMR and revealed that a dipivalate complex was initially formed and slowly converted to catalyst **4** by intramolecular C-H activation of the benzylic position of the *N*-Mes group. It should be noted that C-H activation of the *N*-DIPP group was not observed over the course of the reaction and two possible explanations are envisioned: (1) the benzylic hydrogen on the *N*-DIPP group is highly hindered and would lead to an unstable tertiary carbon- metal bond, and (2) the methyl groups are not activated and the resulting 7-membered chelating architecture is thermodynamically less stable.[16] The crystal structure of complex **4** confirmed formation of this 6-membered chelated structure (Figure 3) and showed essentially the same structural features as catalyst **1a,** except for the obvious change from *N*-Mes to *N*-DIPP.[11a]

In the same manner as **1a**, chelated catalysts bearing bulkier carboxylate ligands were synthesized by the salt metathesis and C-H activation of catalyst **5a**. Reaction of starting complex **5a** with Ag(OCOCMe$_2$Ph) afforded **1b** directly in high yield (Scheme 2). The bulkier salts Ag(OCOCMePh$_2$) and Ag(OCOCPh$_3$) were also reacted with complex **5a** to afford the corresponding NHC-chelated catalysts, however decomposition upon silica gel column chromatography prevented isolation of **1c** and **1d**. In order to synthesize the desired

chelated species, a new synthetic route was devised (Scheme 2). Bistriflate complex **5b** was prepared by treating **5a** with excess AgOTf,[17] and subsequently reacted with sodium carboxylates to provide catalysts **1c** and **1d** cleanly; these species could then be purified by a simple solvent wash. As such, **5b** is a versatile precursor for forming NHC chelated catalysts under mild conditions.[18] In each of these activation reactions, the dicarboxylate complexes are formed as intermediates, followed by intramolecular C-H activation to yield the NHC-chelated catalysts, with concomitant formation of the corresponding carboxylic acids.[19] X-ray crystal structures of catalysts **1b** and **1d** are shown in Figure 4 and display the same structural features as complex **1a**: a 6-membered chelating NHC ligand and an η^2-bound carboxylate ligand with the two oxygen atoms lying in the equatorial plane.

We had previously reported that the pivalate ligand of complex **2a**, bearing a five-membered chelate, could be replaced by a variety of anionic ligands in a facile manner,[11c] however, attempts to exchange the anionic ligand of catalyst **1a** were generally unsuccessful.[20] We were nonetheless able to synthesize an NHC-chelated catalyst substituted with a less bulky chloride ligand. Reaction of complex **1a** with one equivalent of HCl immediately afforded catalyst **6** (Scheme 3). Interestingly, excess HCl caused unchelation of the NHC ligand and provided the dichloride complex **5a**. Presumably, the excess HCl protonated the chelating methylene carbon and broke the ruthenium-carbon bond of **6** while keeping the alkylidene intact. As a result, addition of exactly one equivalent of HCl is required to selectively form complex **6**.

In order to supplement our investigations of chelated catalysts, we investigated some non-chelated analogs containing a single bulky anionic ligand.[21] Recently, Jensen and coworkers reported that a bulky thiolate ligated catalyst derived from catalyst **5a** showed high *cis*-selectivity in simple homocoupling reactions (Figure 5).[10] It was thus proposed that a non-chelated catalyst substituted with a single bulky carboxylate could potentially be *Z*-selective. Initial attempts to synthesize **7a** from **5a** by ligand exchange with one equivalent of AgOPiv were unsuccessful due to formation of a mixture of unreacted **5a** and the bispivalate complex, which subsequently converted to chelated catalyst **1a**. As such, a new synthetic route to this type of nonchelated species was required. Complex **5c** was prepared by treating **5a** with one equivalent of AgOTf.[17] Complex **5c** could then be reacted with sodium carboxylates to yield **7a** (R = Me) and **7d** (R = Ph) in excellent yields (Scheme 4). It should be noted that **7a** and **7d** did not undergo intramolecular C-H activation. Considering that C-H activation and subsequent formation of a chelated structure was observed when the bistriflate complex **5b** was exposed to sodium carboxylates as shown in Scheme 1, it seems that substitution with two carboxylate ligands is required for C-H activation to occur. It is proposed that the congested environment around the ruthenium center in the dicarboxylate intermediate positions one of the carboxylate ligands close enough to interact with the benzylic position of the mesityl group to promote a C-H activation event. The X-ray crystal structure of **7d** is shown in Figure 6. In contrast to the aforementioned chelated catalysts, the carboxylate ligand of **7d** is coordinated to the ruthenium center in a monodentate fashion as a formal 16e- complex, similar to catalyst **5a**.

Ligand Effects on Metathesis Reactivity

The standard CM reaction of allylbenzene (**8**) and *cis*-1,4-diacetoxy-2-butene (**9**) was carried with catalysts **1a-7d** under using previously reported conditions.[22] This reaction provided a good general method to directly compare the catalysts under investigation (Table 1).

Catalyst **4**, bearing the bulkier *N*-DIPP group, showed slightly higher conversion compared to catalyst **1a**, but their trends were quite similar (Figure 7). After reaching a plateau at 60–

70% conversion, the *E*/*Z* ratios remained relatively unchanged over time (Figure 7(b)). It is thought that this is due to the propensity of catalysts **1a** and **4** to decompose under the reaction conditions, preventing metathesis events from isomerizing the *Z*-olefins to the *E*-isomer.[23] Despite reaching similar conversions, differences in stereoselectivity were quite obvious between these two catalysts. Catalyst **4** provided a noticeably lower *E*/*Z* ratio of cross product **10** (49% *E*) compared to catalyst **1a** (59% *E*) at ~ 60% conversion (Figure 7(b)). The higher *Z*-selectivity of **4** compared to **1a** can be explained as follows: because the ruthenacyclobutane forms side-bound and is thus located below the *N*-aryl group, the bulkier *N*-DIPP group repels the substituent in the intermediate leading to *E*-olefin formation (R^1 in Figure 8) more strongly than the smaller *N*-Mes group of **1a**, contributing to the higher Z-selectivity (Figure 8).[25]

In order to further explore the effect of the bulkier *N*-aryl group on *Z*-selectivity, the metathesis homocoupling of substrate **8** (Table 2), and macrocyclic RCM reactions (Table 3) were attempted. As expected from the CM assay above, catalyst **4** exhibited higher *Z*-selectivity compared to **1a** in both assays. In addition, catalyst **4** was superior to **1a** in terms of selectivity for the desired homocoupled product **11** compared to the undesired isomerization product **12**. In contrast to catalyst **1a**, catalyst **4** reached a much higher ratio of **11**/**12** and maintained a high value even when the conversion reached a plateau at 120 minutes. Since the isomerization results from decomposed catalyst, the greater stability of **4** appears to arise from the bulky *N*-DIPP group of **4**.[27]

The effect of the anionic ligand was evaluated by comparing the activity of catalysts **1a-d** bearing increasingly bulkier carboxylate ligands in the standard CM reaction (Figure 9); the steric effects of these anionic ligands can be visualized from the crystal structures of the corresponding catalysts in Figure 4. As shown in Figure 9(a), all of the presented catalysts showed similar trends in conversion, reaching a plateau at around 60% within 30–90 minutes, however the stereoselectivity varied dramatically depending on the identity of the carboxylate ligand (Figure 9(b)). Proceeding from catalyst **1a** to **1d**, as the carboxylate ligand becomes bulkier, the *E*/*Z* ratio increases. Taking into account the side-bound intermediates proposed for **1a** and **2a**,[14] plausible metallacyclobutane intermediates are presented (Figure 10). It is envisioned that the bulkier carboxylate ligand (i.e. Ph_3CCOO (**1d**)) repels the metallacyclobutane substituents (R^1 and R^2 in Figure 10), destabilizing the ruthenacyclobutane intermediate that leads to productive formation of *Z*-olefins (Figure 10(b)) when compared to the less bulky pivalate ligand (i.e. ^{t}BuCOO (**1a**), Figure 10(a)). In the future design of *Z*-selective catalysts containing six-membered chelates, it is envisioned that substitution with less bulky ligands capable of binding in an η^2-fashion will lead to improved catalysts.

Next, we briefly investigated the effects of substituting a chelated catalyst with a monodentate chloride ligand. Despite containing a chelating architecture that normally imparts improved *Z*-selectivity, catalyst **6** provided a high *E*/*Z* ratio of cross product **10** in the standard CM assay (Table 1). The *E*/*Z* ratio was significantly higher than chelated catalyst **1a**, and more closely resembled that of non-chelated ruthenium metathesis catalysts like **5a**. One possible explanation for this is that CM reactions catalyzed by **6** could proceed not via a side-bound intermediate (Figure 11(a)) as proposed for *Z*-selective catalysts **1a** and **2a-b**, but via a bottom-bound ruthenacyclobutane intermediate (Figure 11(b)) as proposed for non-chelated catalysts.[28] In the bottom-bound intermediate, the ruthenacyclobutane substituents (R^1 and R^2 in Figure 11) would be located farther away from the NHC ligand, meaning that there would be less steric influence on the substituents, seemingly providing the thermodynamically preferred *E*-isomer. Given the lack of experimental and theoretic evidence, this hypothesis is conjecture at this point.

Previously, Jensen and coworkers reported that a non-chelated catalyst bearing a single bulky thiolate ligand (Figure 5) catalyzed highly *Z*-selective olefin metathesis and proceeded through a bottom-bound ruthenacyclobutane intermediate.[10b] Catalysts **7a** and **7d** bearing a single bulky carboxylate ligand were therefore prepared and tested in the standard CM assay. The trends in stereoselectivity for the non-chelated catalysts **7a** and **7d** were very similar to that of catalyst **5a**, favoring formation of the *E*-isomer (Figure 12(b)). Clearly, the presence of a single carboxylate ligand does not lead to any observable *Z*-selectivity. It is envisioned that CM reactions catalyzed by **7a** and **7d** proceed via bottom-bound ruthenacyclobutane intermediates (Figure 13(b)), however the carboxylate ligand does not seem bulky enough to force the ruthenacyclobutane substituents (R^1 and R^2 in Figure 13) in the same direction to productively form *Z*-olefin products. Even if these catalysts proceeded via side-bound intermediates (Figure 13(a)), because of free rotation around the Ru-C(NHC) bond which is allowed in non-chelated structures, the *N*-Mes group of the NHC ligand cannot effectively repel the ruthenacyclobutane substituents. Either way, the thermodynamically favored *E*-isomer dominates in reactions catalyzed by **7a** and **7d**.

CONCLUSION

In summary, we have synthesized a series of catalysts containing six-membered chelating architectures and their non-chelated analogs, and determined their performance in various olefin metathesis assays. From these studies, new information has been gained about how changes to the NHC and anionic ligand affect a catalyst's *Z*-selectivity. In designing a highly efficient *Z*-selective catalyst, understanding the roles of each ligand on a catalyst's reactivity and selectivity is very useful. It was shown that catalysts require I) an NHC-chelated structure and II) an η^2-bound carboxylate ligand to maintain high levels of *Z*-selectivity. When the bidentate pivalate ligand on catalyst **1a** was replaced with a monodentate chloride (**6**), there was a marked decrease in *Z*-selectivity. Additionally, as demonstrated with catalyst **4**, a bulky *N*-aryl group enhances *Z*-selectivity due to increased steric repulsion with ruthenacyclobutane substituents. As was previously shown, these NHC-chelated structures lock rotation of the NHC ligand and force the *N*-aryl group above the ruthenacyclobutane, allowing it to better influence it's substituents and favoring formation of a *cis*-disubstituted ruthenacycle in order to productively form *Z*-olefins. In considering the difference in selectivity between catalysts **1a-1d** bearing carboxylate ligands of different sizes, a less bulky η^2-ligand seems to promote higher *Z*-selectivity, presumably because it enables more effective repulsion from the *N*-aryl group. In order to design highly *Z*-selective catalysts with a six-membered chelated architecture, catalyst activity and selectivity must be improved to compliment the family of five-membered chelated catalysts.

Supplementary Material

Refer to Web version on PubMed Central for supplementary material.

Acknowledgments

We thank Dr. D. Benitez, Dr. B. K. Keitz and Dr. P. Teo for helpful discussions and suggestions for this work. Materia, Inc. is thanked for the generous donation of catalysts. Dr. M. W. Day and Mr. L. M. Henling are acknowledged for X-ray crystallography analysis. The Bruker KAPPA APEXII X-ray diffractometer was purchased via an NSF CRIF:MU award to the California Institute of Technology, CHE-0639094. This work was financially supported by National Institutes of Health (NIH 5R01GM031332-27) and Mitsui Chemicals, Inc.

REFERENCES

1. Cossy, J.; Arseniyadis, S.; Meyer, C. Metathesis in Natural Product Synthesis: Strategies, Substrates, and Catalysts. 1st ed. Weinheim, Germany: Wiley-VCH; 2010.

2. Binder JB, Raines RT. Curr. Opin. Chem. Biol. 2008; 12:767. [PubMed: 18935975]
3. Schrodi Y, Ung T, Vargas A, Mkrtumyan G, Lee CW, Champagne TM, Pederson RL, Hong SH. CLEAN - Soil, Air, Water. 2008; 36:669.
4. (a) Leitgeb A, Wappel J, Slugovc C. Polymer. 2010; 51:2927.(b) Sutthasupa S, Shiotsuki M, Sanda F. Polymer Journal. 2010; 42:905.(c) Liu X, Basu A. J. Organomet. Chem. 2006; 691:5148.
5. Fürstner A. Angew. Chem. Int. Ed. 2000; 39:3012.
6. Schrock RR, Hoveyda AH. Angew. Chem. Int. Ed. 2003; 42:4592.
7. (a) Trnka TM, Grubbs RH. Acc. Chem. Res. 2001; 34:18. [PubMed: 11170353] (b) Samojlowicz C, Bieniek M, Grela K. Chem. Rev. 2009; 109:3708. [PubMed: 19534492] (c) Vougioukalakis G, Grubbs RH. Chem. Rev. 2010; 110:1746. [PubMed: 20000700]
8. Grubbs, RH., editor. Handbook of Metathesis. Vol. Vols. 1–3. Weinheim: Wiley-VCH; 2003.
9. (a) Flook MM, Jiang AJ, Schrock RR, Müller P, Hoveyda AH. J. Am. Chem. Soc. 2009; 131:7962. [PubMed: 19462947] (b) Jiang AJ, Zhao Y, Schrock RR, Hoveyda AH. J. Am. Chem. Soc. 2009; 131:16630. [PubMed: 19919135] (c) Marinescu SC, Schrock RR, Müller P, Takase MK, Hoveyda AH. Organometallics. 2011; 30:1780. [PubMed: 21686089] (d) Meek SJ, O'Brien RV, Llaveria J, Schrock RR, Hoveyda AH. Nature. 2011; 471:461. [PubMed: 21430774] (e) Flook MM, Ng VWL, Schrock RR. J. Am. Chem. Soc. 2011; 132:1784. [PubMed: 21265524] (f) Yu M, Wang C, Kyle AF, Jukubec P, Dixon DJ, Schrock RR, Hoveyda AH. Nature. 2011; 479:88. [PubMed: 22051677] (g) Townsent EM, Schrock RR, Hoveyda AH. J. Am. Chem. Soc. 2012; 134:11334. [PubMed: 22734508] (h) Wang C, Haeffner F, Schrock RR, Hoveyda AH. Angew. Chem. Int. Ed. 2013; 52:1939.(i) Wang C, Yu M, Kyle AF, Jakubec P, Dixon DJ, Schrock RR, Hoveyda AH. Chem. Eur. J. 2013; 19:2726. [PubMed: 23345004]
10. (a) Occhipinti G, Hansen FR, Törnroos KW, Jensen VR. J. Am. Chem. Soc. 2013; 135:3331. [PubMed: 23398276] (b) Jensen VR, Occhipinti G, Hansen FR. Novel Olefin Metathesis Catalysts Int. Patent Appl. WO 2012032131. 2012
11. (a) Endo K, Grubbs RH. J. Am. Chem. Soc. 2011; 133:8525. [PubMed: 21563826] (b) Keitz BK, Endo K, Herbert MB, Grubbs RH. J. Am. Chem. Soc. 2011; 133:9686. [PubMed: 21649443] (c) Keitz BK, Endo K, Patel PR, Herbert MB, Grubbs RH. J. Am. Chem. Soc. 2012; 134:693. [PubMed: 22097946] (d) Rosebrugh LE, Herbert MB, Marx VM, Keitz BK, Grubbs RH. J. Am. Chem. Soc. 2013; 135:1276. [PubMed: 23317178]
12. (a) Trnka TM, Morgan JP, Sanford MS, Wilhelm TE, Scholl M, Choi TL, Ding S, Day MW, Grubbs RH. J. Am. Chem. Soc. 2003; 125:2546. [PubMed: 12603143] (b) Leitao EM, Dubberley SR, Piers WE, Wu Q, McDonald R. Chem. Eur. J. 2008; 14:11565. [PubMed: 19035588]
13. (a) Herbert MB, Marx VM, Pederson RL, Grubbs RH. Angew. Chem. Int. Ed. 2013; 52:310.(b) Marx VM, Herbert MB, Keitz BK, Grubbs RH. J. Am. Chem. Soc. 2013; 135:94. [PubMed: 23244210]
14. (a) Liu P, Xu X, Dong X, Keitz BK, Herbert MB, Grubbs RH, Houk KN. J. Am. Chem. Soc. 2012; 134:1464. [PubMed: 22229694] (b) Dang Y, Wang ZX, Wang X. Organometallics. 2012; 31:7222. (c) Dang Y, Wang ZX, Wang X. Organometallics. 2012; 31:8654.(d) Miyazaki H, Herbert MB, Liu P, Dong X, Xu X, Keitz BK, Ung T, Mkrtumyan G, Houk KN, Grubbs RH. J. Am. Chem. Soc. 2013; 135:5848. [PubMed: 23547887]
15. We recently reported that an intramolecular C-H bond activation for adamantyl analogue **2c** could be achieved only when sodium pivalate was used. See ref. 11d.
16. When $[H_2I(DIPP)_2]RuCl_2[=CH\text{-}o\text{-}(O^iPr)C_6H_4]$ was reacted with silver pivalate, a complex bearing two pivalte ligands was formed but no intramolecular C-H bond activation was observed even upon heating.
17. **5b** and **5c** were synthesized by modification of reported procedure: Krause JO, Nuyken O, Wurst K, Buchmeiser MR. Chem. Eur. J. 2004; 10:777. [PubMed: 14767943]
18. A mild method to effect the salt metathesis and C-H activation directly using NaOPiv was recently reported (ref 11d). However, a reaction of **5a** with NaOAc only led to catalyst decomposition. This result may suggest that bulky carboxylate is necessary for formation and/or stabilization of the NHC-chelating catalyst.
19. All the acidic protons of the carboxylic acids were detected around δ = 10.5–11.5 ppm in ^{1}H NMR spectra.

20. Attempts to replace the pivalate ligand on catalyst **1a** with a nitrate ligand were unsuccessful.
21. Teo P, Grubbs RH. Organometallics. 2010; 29:6045.
22. Ritter T, Hejl A, Wenzel AG, Funk TW, Grubbs RH. Organometallics. 2006; 25:5740.
23. Reported decomposition pathways for **2a**, in which the alkylidene moiety inserts into the Ru-C bond, followed by hydride elimination, were suggested from isolated decomposed product and supported by computational results (See Ref. 24). It is proposed that reaction intermediates of catalyst with six-membered chelates, including methylidene complexes, tend to suffer from analogous decomposition pathways. Although none of decomposed product was isolated, dramatic color change of the reaction solution from green to yellow were observed for **1a** and **4**, respectively. In RCM of diethyldiallyl malonate and ROMP of 1,5-cyclooctadiene by catalysts **1a** and **4**, conversion also reached a plateau within 15–60 minutes. See detail in SI.
24. Herbert MB, Lan Y, Keitz BK, Liu P, Endo K, Day MW, Houk KN, Grubbs RH. J. Am. Chem. Soc. 2012; 134:7861. [PubMed: 22500642]
25. We have also reported higher *Z*-selectivity for **2c** substituted with an *N*-DIPP group compared to **2b** substituted with an *N*-Mes group. See ref. 11d.
26. (a) Ivin, KJ.; Mol, JC. Olefin Metathesis and Metathesis Polymerization. San Diego, CA: Academic Press; 1997. (b) Pederson RL, Fellows IM, Ung TA, Ishihara H, Hajela S. Adv. Synth. Catal. 2002; 344:728.(c) Lehman SE, Schwendeman JE, O'Donnell PM, Wagener KB. Inorg. Chim. Acta. 2003; 345:190.(d) Schmidt B. Eur. J. Org. Chem. 2004:1865. and references therein.
27. We have also reported that **2c** gave higher proportion of the metathesis product than **2b** in the homocoupling of **8**. See ref 11d.
28. (a) Adlhart C, Chen P. J. Am. Chem. Soc. 2004; 126:3496. [PubMed: 15025477] (b) Cavallo L, Correa A. J. Am. Chem. Soc. 2006; 128:13352. [PubMed: 17031936] (c) Benitez D, Tkatchouk E, Goddard WA III. Chem. Commun. 2008:6194.
29. DFT calculation for **1a, 2a** and **2b** shows that side-bound pathways are energetically more favored than the bottom-bound pathways. See ref. 14.

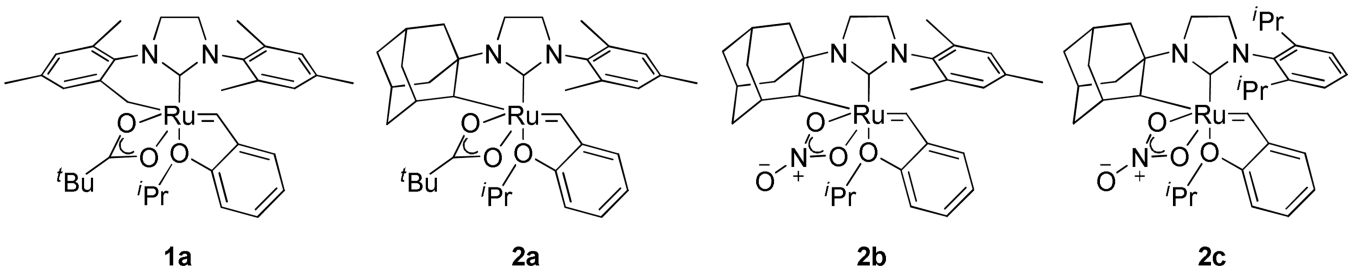

Figure 1.
Ruthenium-based NHC-chelated catalysts for *Z*-selective olefin metathesis.

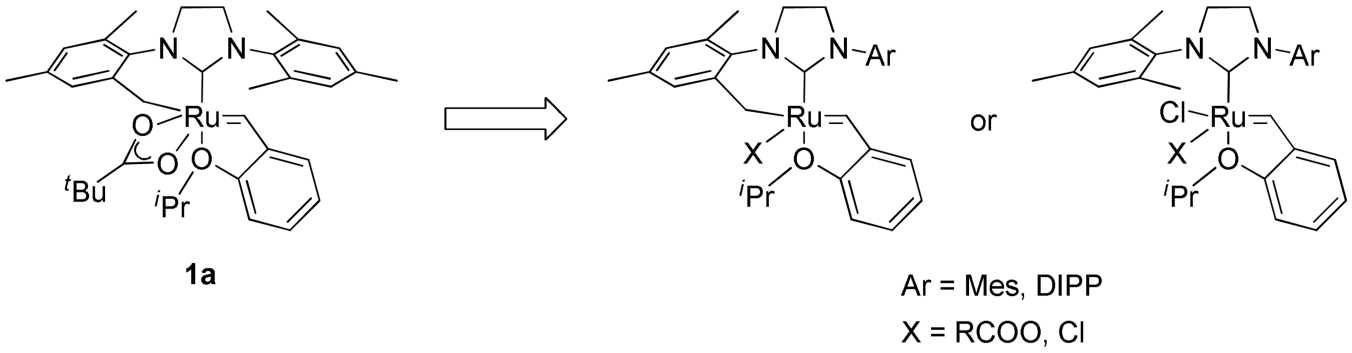

Figure 2.
Proposed modifications to catalyst **1a**. Mes = 2,4,6-trimethylphenyl, DIPP = 2,6-diisopropylphenyl.

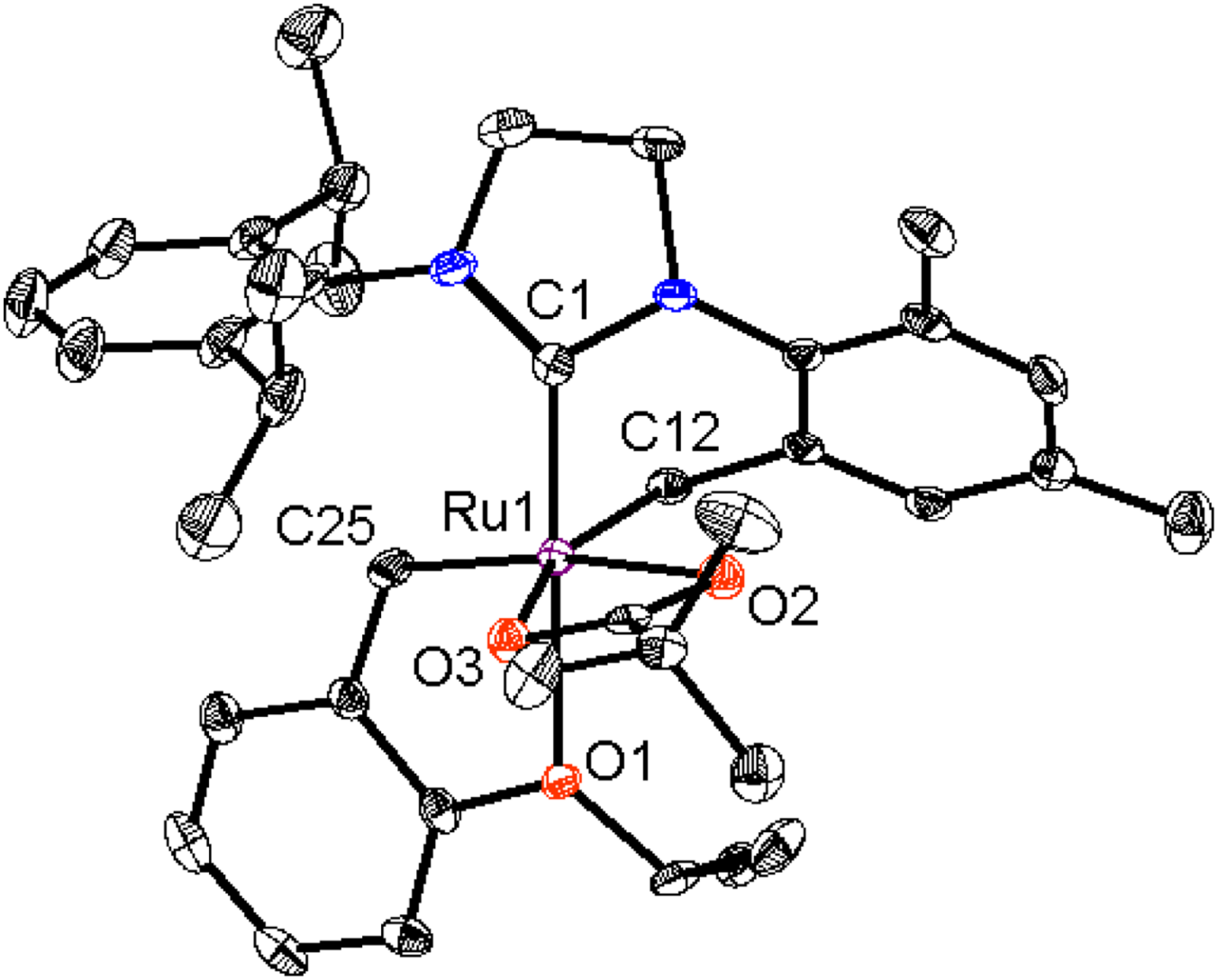

Figure 3.

X-ray crystal structure of catalyst **4** is shown. Displacement ellipsoids are drawn at 50% probability. For clarity, hydrogen atoms have been omitted. Selected bond length (Å) for **4**: C1-Ru1 1.931, C12-Ru1 2.094, C25-Ru1 1.842, O1-Ru1 2.305, O2-Ru1 2.360, O3-Ru1 2.235;

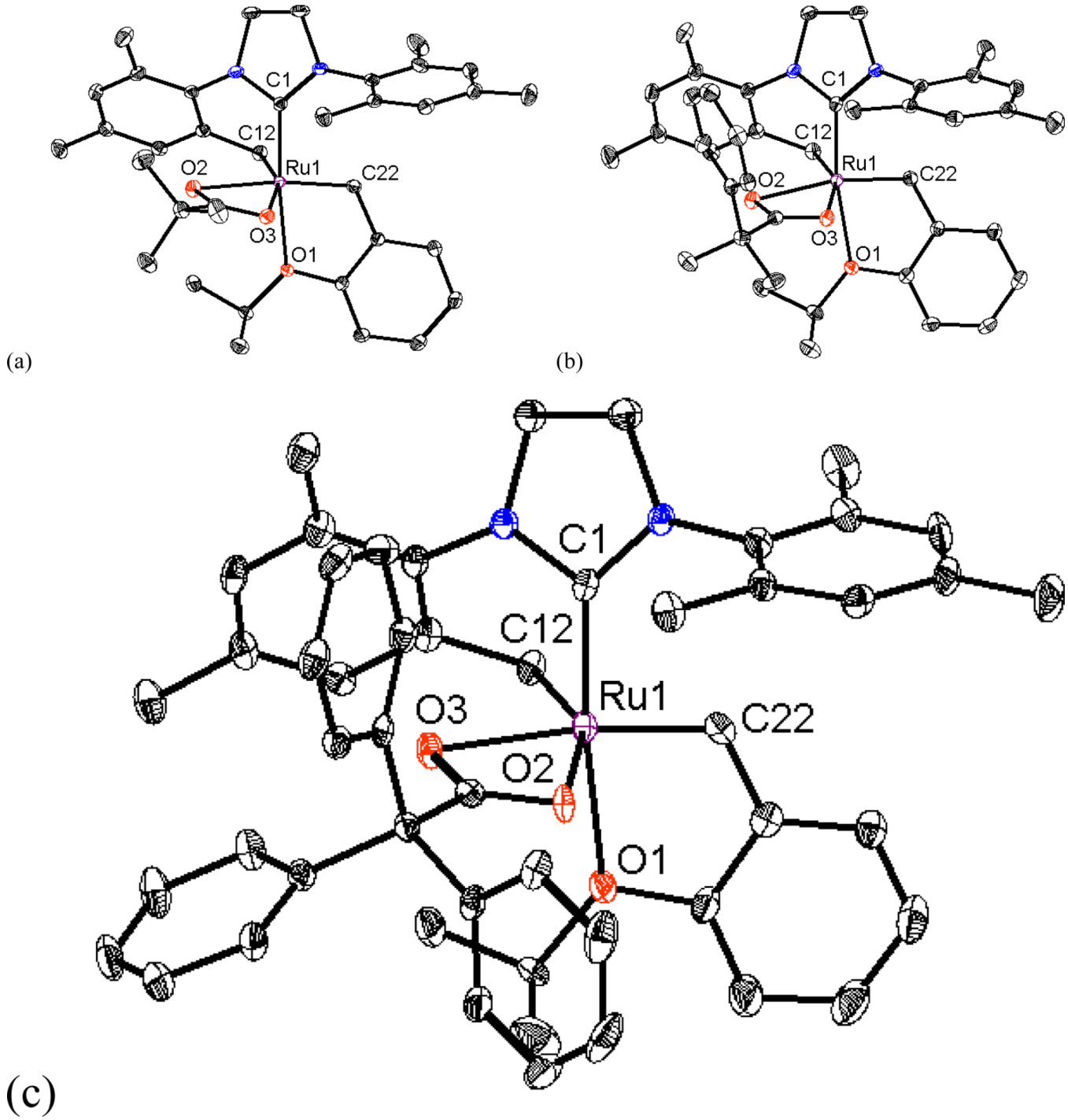

Figure 4.

X-ray crystal structures of catalysts (a) **1a**,[11a] (b) **1b** and (c) **1d** are shown. Displacement ellipsoids are drawn at 50% probability. For clarity, hydrogen atoms have been omitted. Selected bond length (Å) for **1a**: C1-Ru1 1.945, C12-Ru1 2.095, C22-Ru1 1.840, O1-Ru1 2.296, O2-Ru1 2.332, O3-Ru1 2.230; for **1b**: C1-Ru1 1.939, C12-Ru1 2.094, C22-Ru1 1.843, O1-Ru1 2.325, O2-Ru1 2.332, O3-Ru1 2.218; for **1d**: C1-Ru1 1.926, C12-Ru1 2.102, C22-Ru1 1.843, O1-Ru1 2.314, O2-Ru1 2.252, O3-Ru1 2.301.

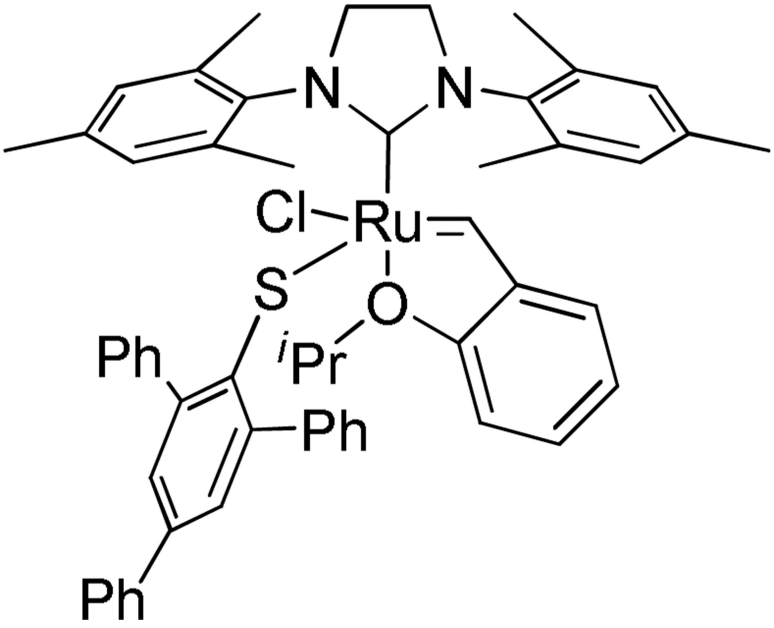

Figure 5.
A reported ruthenium catalyst bearing a bulky thiolate ligand.

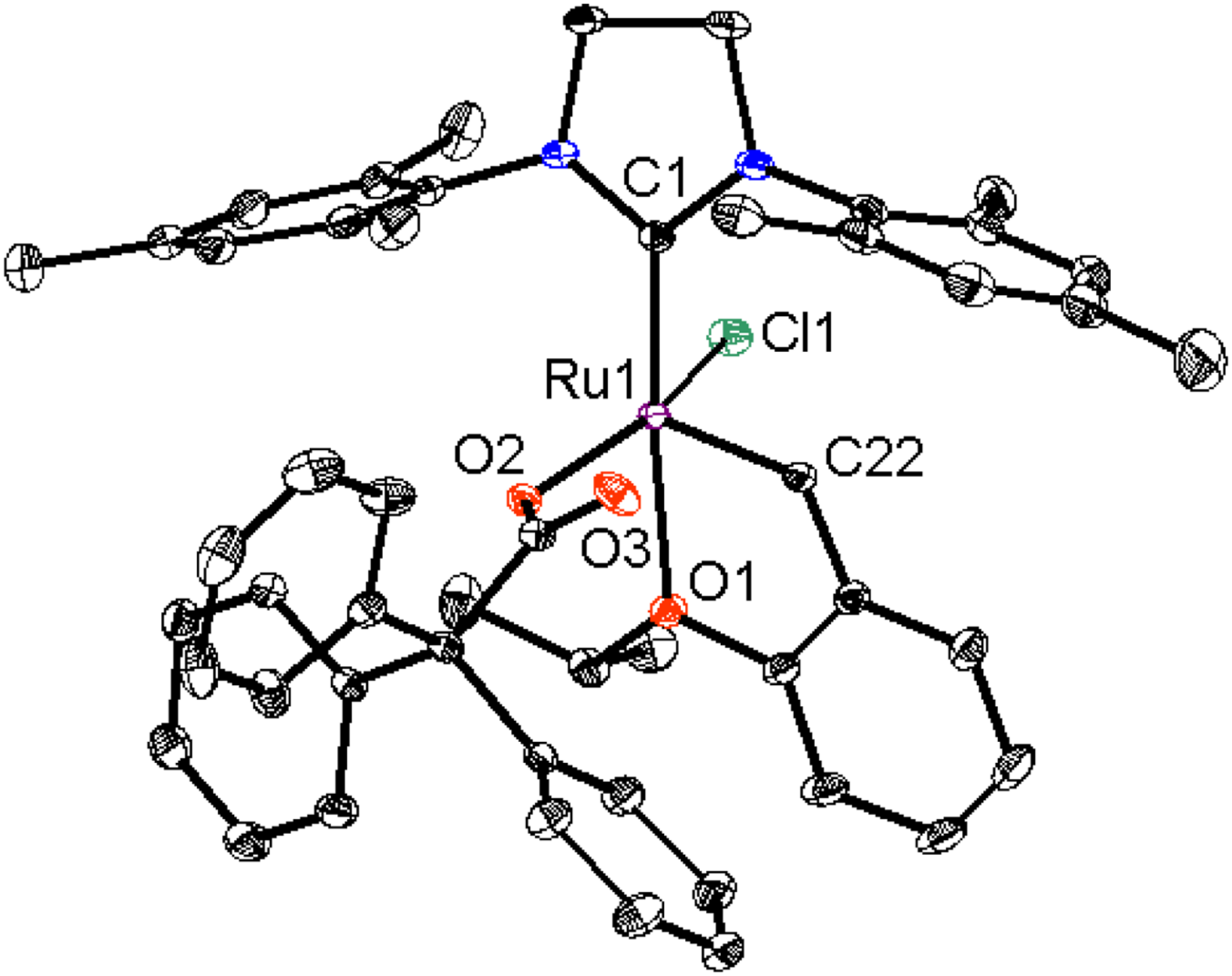

Figure 6.

X-ray crystal structure of catalyst **7d** is shown. Displacement ellipsoids are drawn at 50% probability. For clarity, hydrogen atoms have been omitted. Selected bond length (Å) for **7d**: C1-Ru1 1.975, C22-Ru1 1.830, Cl1-Ru1 2.341, O1-Ru1 2.261, O2-Ru1 2.021.

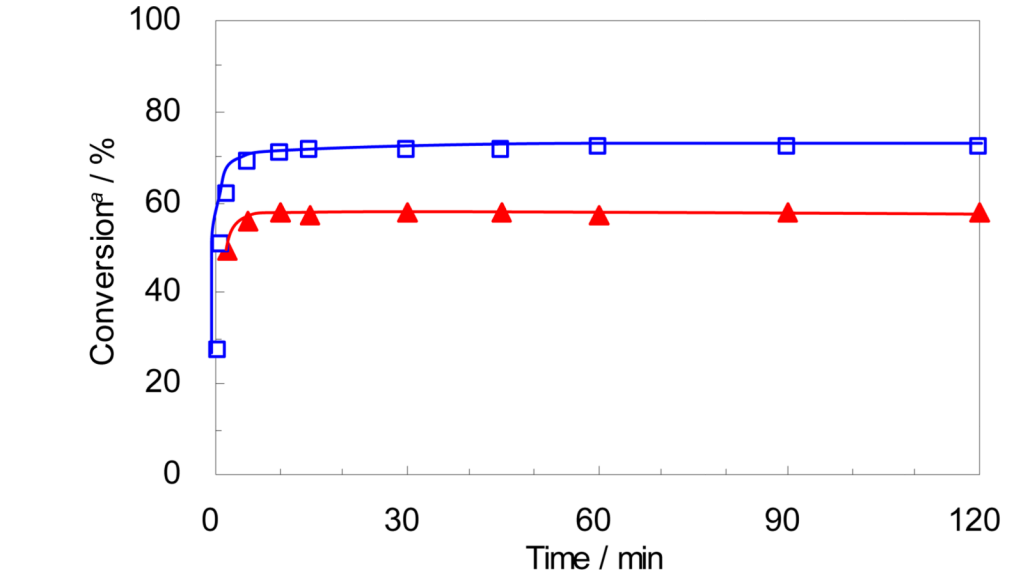

(a)

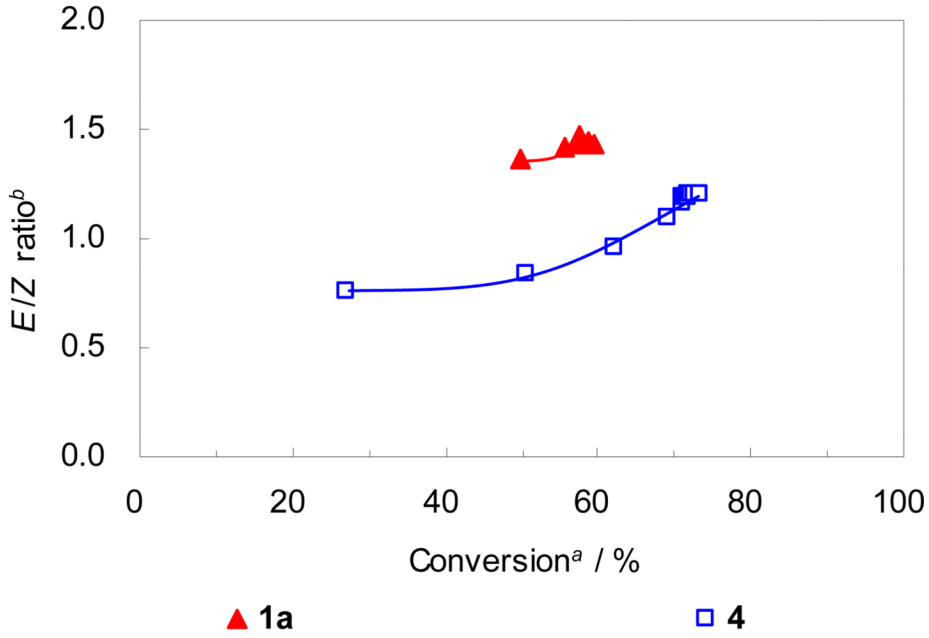

(b)

Figure 7.

Plots for (a) conversion vs time and (b) *E/Z* ratio vs conversion for CM of **8** and **9**. [a] Conversion of **8** to **10** determined by GC analysis. [b] Molar ratio of *E* isomer and *Z* isomer of **10** determined by GC analysis.

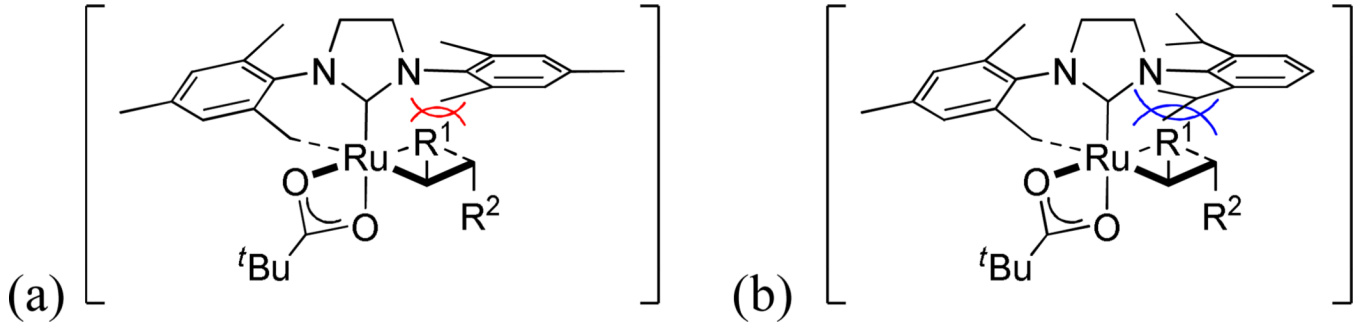

Figure 8.
Plausible side-bound intermediates that lead to *E*-olefins for catalysts (a) **1a** and (b) **4**.

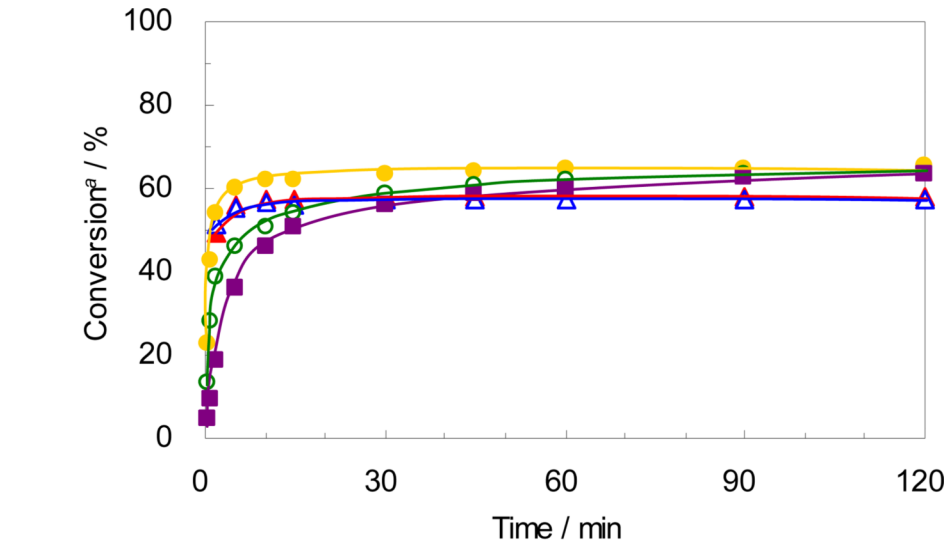

(a)

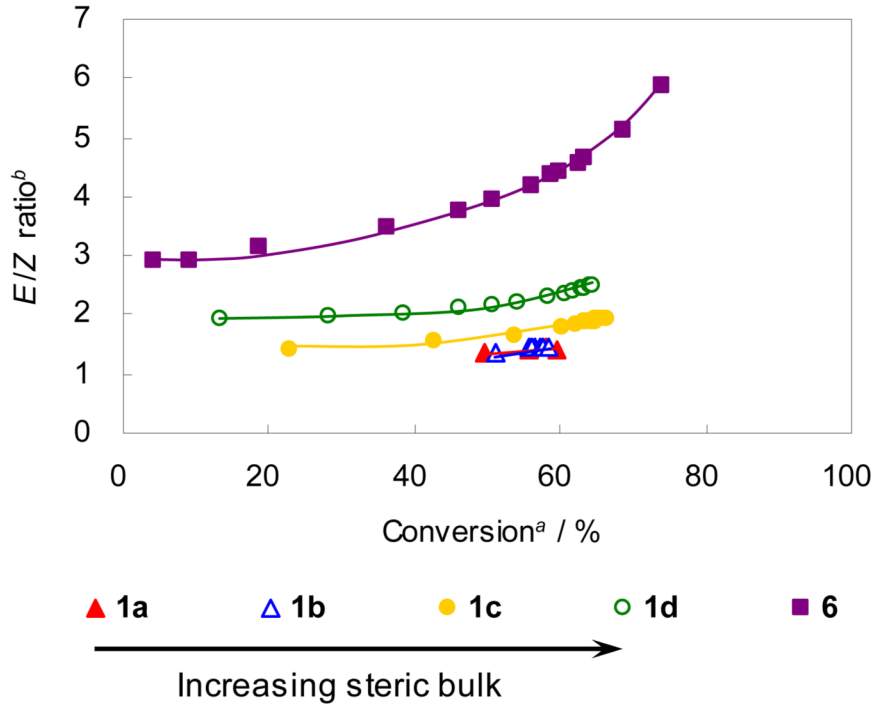

(b)

Figure 9.

Plots for (a) conversion vs time and (b) *E/Z* ratio vs conversion for CM of **8** and **9**. [a] Conversion of **8** to **10** determined by GC analysis. [b] Molar ratio of *E* isomer and *Z* isomer of **10** determined by GC analysis.

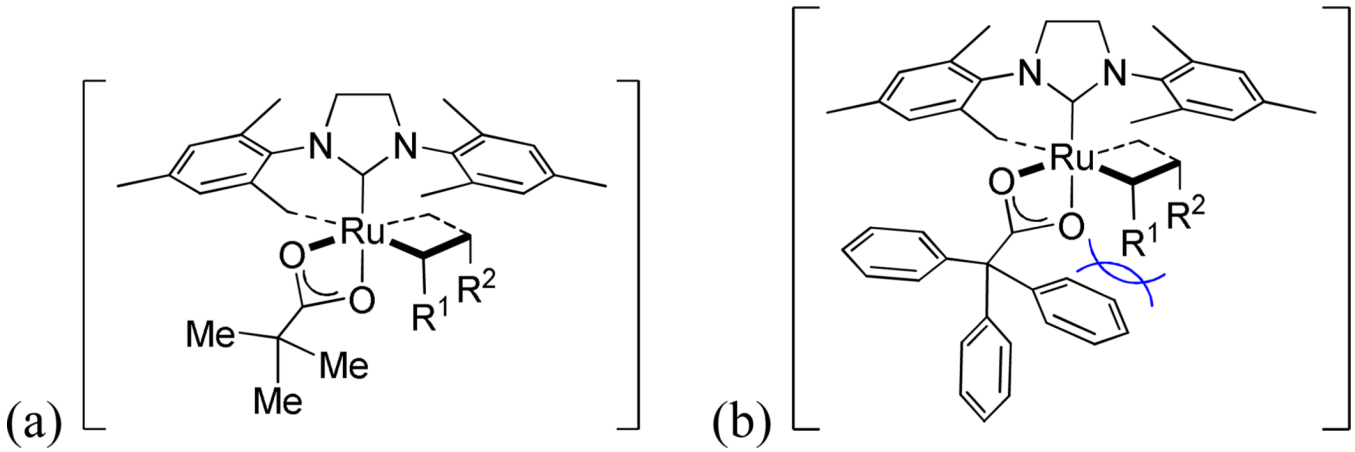

Figure 10.
Plausible side-bound intermediates for (a) **1a** and (b) **1d**.

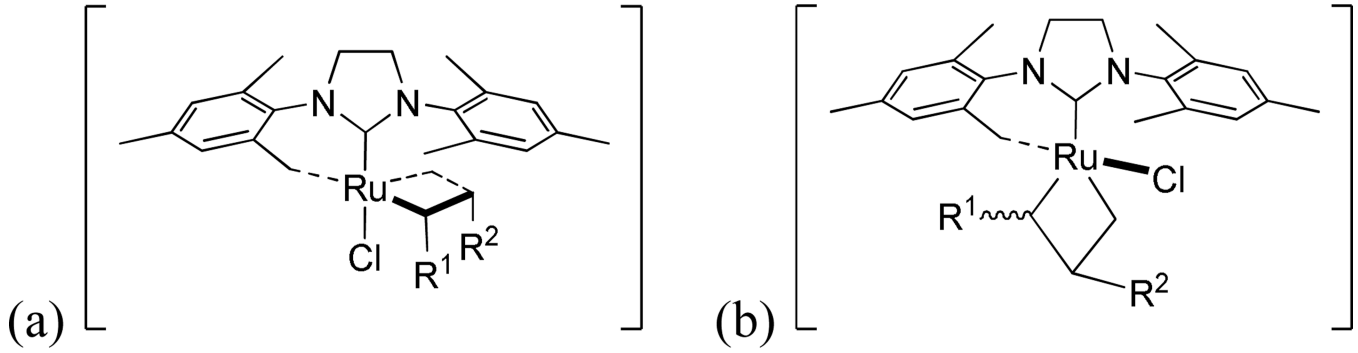

Figure 11.
Possible side-bound intermediate (a) and bottom-bound intermediate (b) for **6**.

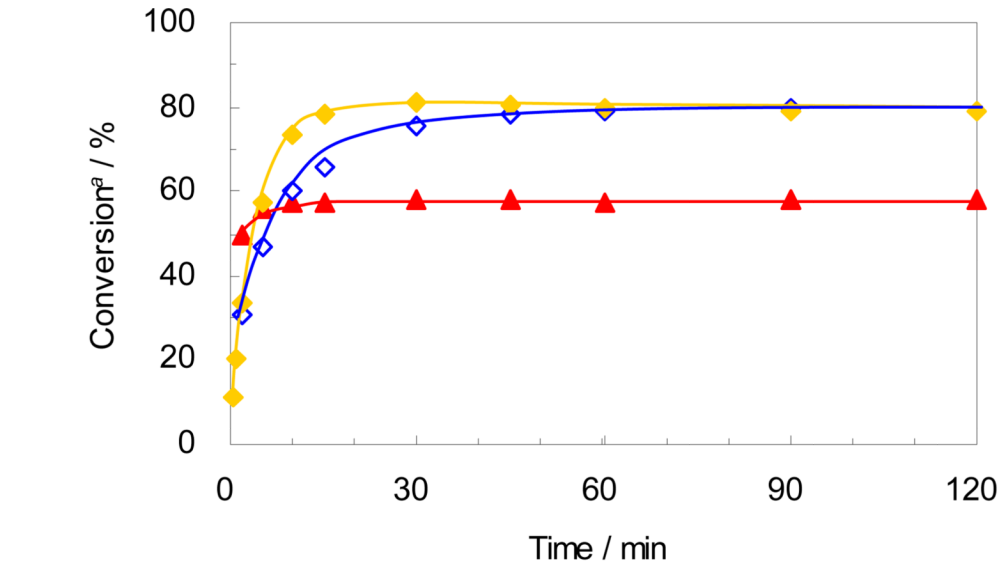

(a)

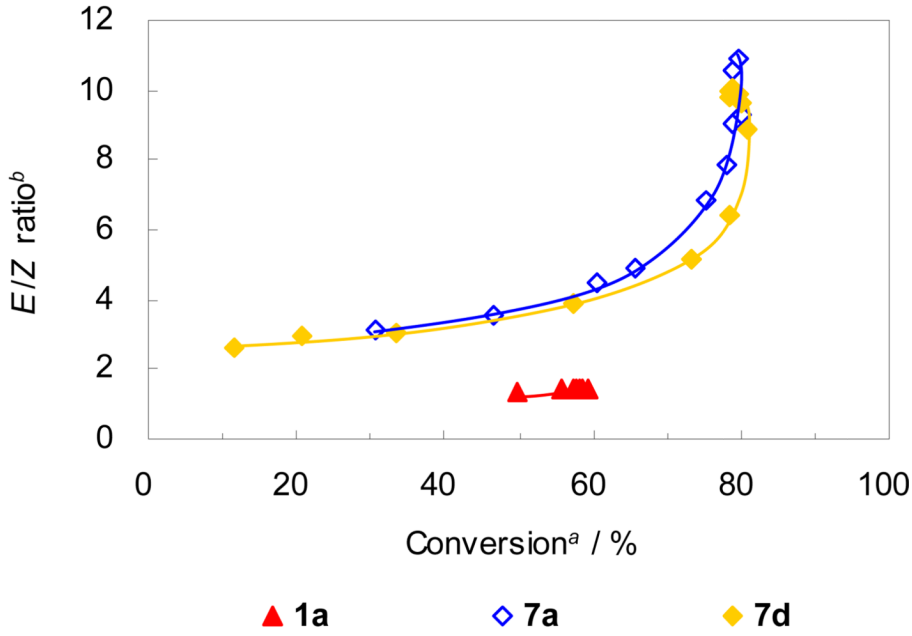

(b)

Figure 12.

Plots for (a) conversion vs time and (b) *E/Z* ratio vs conversion for CM of **8** and **9**. [a] Conversion of **8** to **10** determined by GC analysis. [b] Molar ratio of *E* isomer and *Z* isomer of **10** determined by GC analysis.

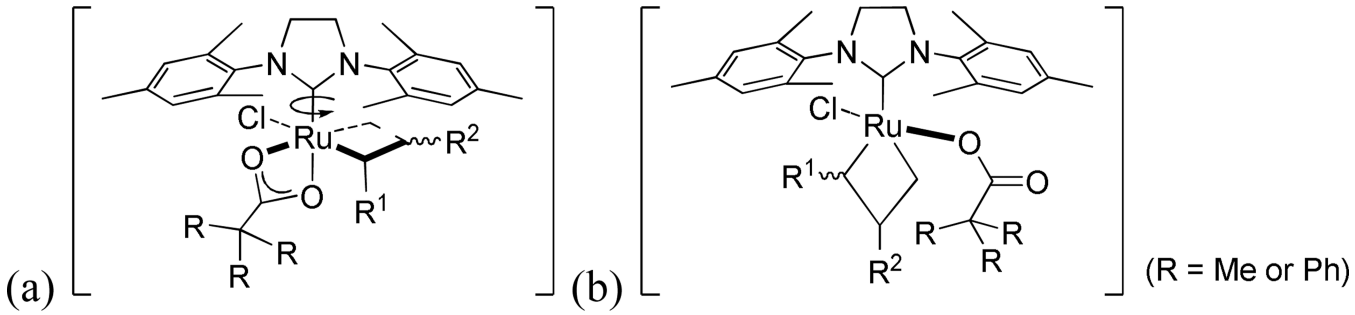

Figure 13.
Possible (a) side-bound intermediate and (b) bottom-bound intermediate for **7a** and **7d**.

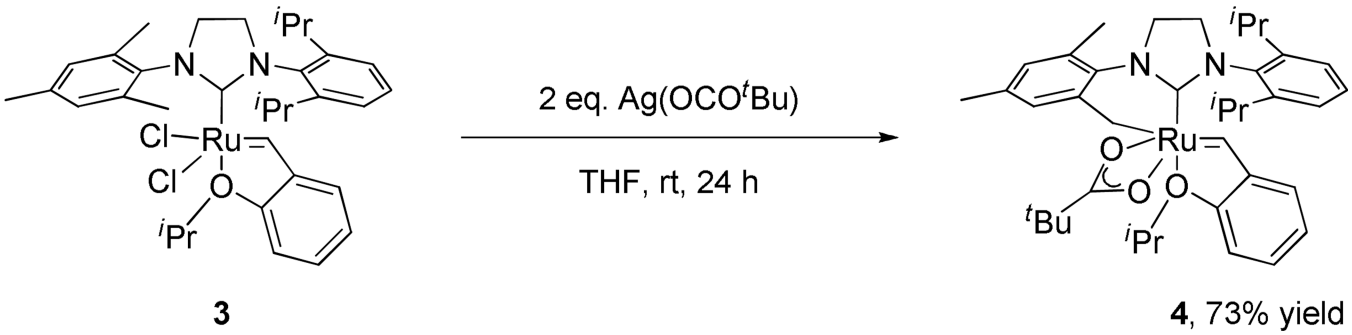

3 **4**, 73% yield

Scheme 1.
Synthesis of NHC-chelated catalyst **4**

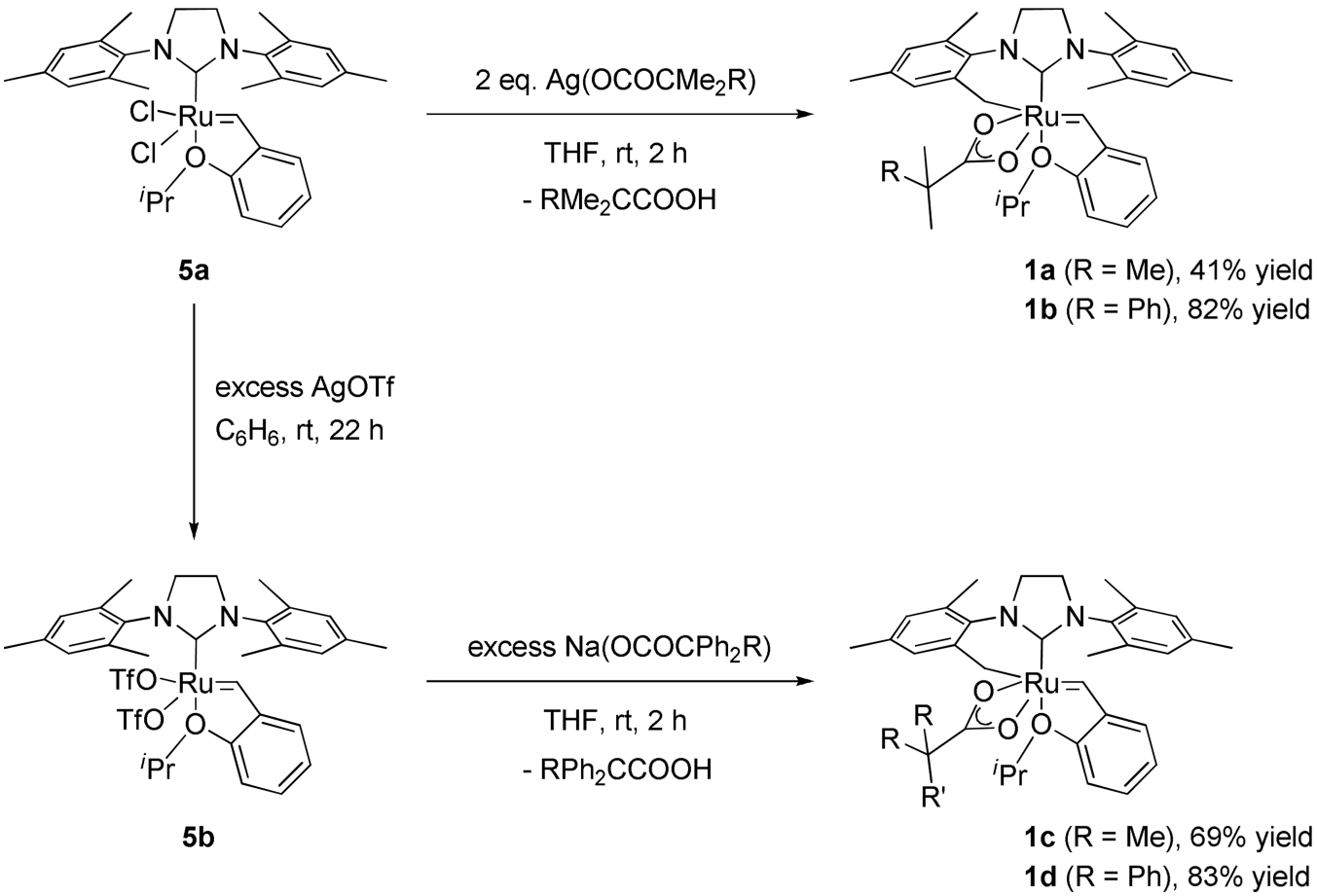

Scheme 2.
Syntheses of NHC-chelated catalysts **1a-d**

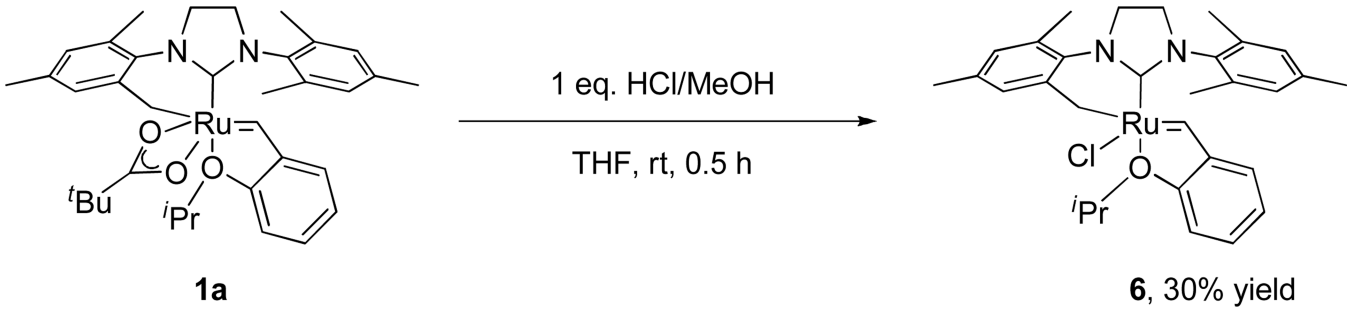

Scheme 3.
Synthesis of NHC-chelated catalyst **6**

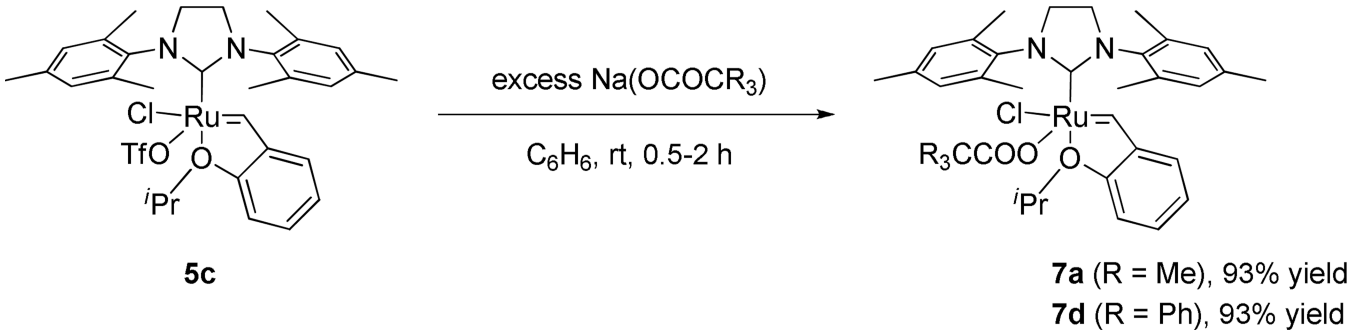

Scheme 4.
Syntheses of non-chelated catalysts **7a** and **7d**

Table 1

Selected data for the CM of **8** and **9** [a]

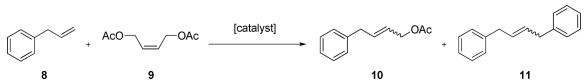

					10		11	
entry	**cat.**	**cat. load., mol %[b]**	**solvent**	**time, min**	**conv, %[c]**	***E* /*Z* [d]**	**conv, %[c]**	***E* /*Z* [d]**
1[e]	**1a**	2.5	C_6H_6	2	50	1.4	2.8	0.75
				30	58	1.5	3.1	1.4
2	**1b**	2.5	C_6H_6	2	51	1.3	2.2	0.79
				30	57	1.5	2.7	0.75
3	**1c**	2.5	C_6H_6	2	54	1.6	2.0	1.4
				30	63	1.9	3.1	1.2
4	**1d**	2.5	C_6H_6	2	39	2.0	(NA)[f]	(NA)[f]
				30	58	2.3	2.9	1.3
5	**3**	2.5	C_6H_6	2	70	4.1	5.4	3.4
				30	84	9.1	8.3	6.5
6	**4**	2.5	C_6H_6	2	62	0.95	3.0	0.94
				30	72	1.2	4.7	1.0
7[e]	**5a**	2.5	C_6H_6	2	70	11	7.6	6.0
				30	66	11	10	6.9
8	**6**	2.5	C_6H_6	2	19	3.2	(NA)[f]	(NA)[f]
				30	56	4.2	1.3	5.3
9	**7a**	2.5	C_6H_6	2	31	3.1	2.1	2.7
				30	75	6.8	7.0	6.5
10	**7d**	2.5	C_6H_6	2	33	3.1	1.0	2.2
				30	81	8.9	7.5	5.3

[a] All reactions were carried out using 0.005 mmol of catalyst, 0.20 mmol of **8**, 0.40 mmol of **9** and 0.10 mmol of tridecane (internal standard for GC analysis) in 1.0 ml of C_6H_6 at 23°C.

[b] Based on **8**.

[c] Conversion of **8** to the product determined by GC analysis.

[d] Molar ratio of *E* isomer and *Z* isomer of the product determined by GC analysis.

[e] Ref. 10a.

[f] GC signal of the product was too small to quantify.

Table 2

Selected data for the metathesis homocoupling of **8** [a]

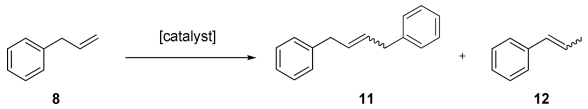

					11		11/12[e]
entry	**cat.**	**cat. load., mol %[b]**	**solvent**	**time, min**	**conv, %[c]**	***E/Z* [d]**	
1	**1a**	2.5	C_6H_6	15	25	0.97	13
				120	32	1.4	2.9
2	**4**	2.5	C_6H_6	45	24	0.97	26
				120	29	1.1	19

[a] All reactions were carried out using 0.005 mmol of catalyst, 0.20 mmol of **8** and 0.10 mmol of tridecane (internal standard for GC analysis) in 1.0 ml of C_6H_6 at 23°C.

[b] Based on **8**.

[c] Conversion of **8** to **11** determined by GC analysis.

[d] Molar ratio of *E* isomer and *Z* isomer of **11** determined by GC analysis.

[e] Determined by GC analysis.

Table 3

Selected data for the macrocyclic RCM of **16** [a]

13 **14**

					14	
entry	**cat.**	**cat. load., mol %[b]**	**solvent**	**time, min**	**conv, %[c]**	***E*/*Z*[d]**
1	**1a**	5.0	C_6H	30	17	1.1
				120	24	1.1
2	**4**	5.0	C_6H_6	30	12	0.77
				120	19	0.83

[a] All reactions were carried out using 0.003 mmol of catalyst, 0.060 mmol of **13** and 0.10 mmol of tridecane (internal standard for GC analysis) in 20 ml of C_6H_6 at 50°C.

[b] Based on **13**.

[c] Conversion of **13** to **14** determined by GC analysis.

[d] Molar ratio of *E* isomer and *Z* isomer of **14** determined by GC analysis.